resistance against pathogens and parasites in animals is scarce, and comes largely from studies on populations of farm or laboratory animals with highly modified genetic backgrounds (reviewed in ref. 1). Finally, because of the enormous amount known about *Drosophila* genetics, we suggest that the interactions between *D. melanogaster* and *A. tabida* may be a valuable model system for the study of the evolution of resistance and of the genetic basis of adaptation.   □

Methods

Competitive ability of selected and control lines. Competitive ability was assessed by placing 15 second-instar larvae from the experimental lines (either control or selected insects) with 15 second-instar larvae from the tester stock (sparkling poliert, an eye-colour mutant) in agar-lined Petri dishes with variable amounts of larval medium. Four food levels were used: 0.4, 0.2, 0.1 or 0.05 ml of larval medium (25 g live baker's yeast per 100 ml water), which represent weak to strong competition regimes. We recorded the number of experimental and tester flies that survived, the development time to pupation and to adult eclosion, and female size and fluctuating asymmetry (wing length). We performed 15 replicates of each combination of line and food level.
Data analysis. Survival data were analysed using both a robust competition index (I) and a more sophisticated analysis using generalized linear modelling techniques (II). For analysis (I) we calculated the competition index[15], $\log(e/(t+1))$, where e is the number of experimental and t is the number of tester flies that survived in each replicate. The means of the competition index for the eight lines were calculated and differences between selected and control lines tested using the t-test with unequal variances. For analysis (II) the untransformed survival data for the experimental flies were analysed in a generalized linear model with binomial error variances, but using quasi-likelihood estimation to account for overdispersion[17]. The numbers of tester flies surviving was used as a covariate and significance assessed by nesting lines within control or selection treatments (giving an F-statistic with one and six degrees of freedom). Examination of the distribution of residuals supported the choice of model. The results of the two statistical analyses were in broad agreement (values in the text are from analysis (II)), with P for (I) given first: 0.4 ml, $P > 0.1$, $P > 0.1$; 0.2 ml, $P > 0.1$, $P > 0.1$; 0.1 ml, $P = 0.033$, $P = 0.011$; 0.05 ml, $P = 0.066$, $P = 0.061$. The data for size and development time were analysed using the appropriate general linear models equivalent to analysis (II).

1. Read, A. F. *et al.* in *Ecology of Infectious Diseases in Natural Populations* (eds Grenfell, B. T. & Dobson, A. P.) 450–477 (Cambridge Univ. Press, 1995).
2. Partridge, L. & Fowler, K. Direct and correlated responses to selection on age at reproduction in *Drosophila melanogaster. Evolution* **46,** 76–91 (1992).
3. Rose, M. R. Laboratory evolution of postponed senescence in *Drosophila melanogaster. Evolution* **38,** 1004–1010 (1984).
4. Salt, G. *The Cellular Defence Reactions of Insects* (Cambridge Univ. Press, 1970).
5. Gupta, A. P. in *Comprehensive Insect Physiology, Biochemistry and Pharmacology*, Vol. 3 (eds Kerkut, G. A. & Gilbert, L. I.) 401–451 (Pergamon, Oxford, 1985).
6. Strand, M. R. & Pech, L. L. Immunological basis for compatibility in parasitoid-host relationships. *Annu. Rev. Entomol.* **40,** 31–56 (1995).
7. Godfray, H. C. J. *Parasitoids, Behavioral and Evolutionary Ecology,* (Princeton Univ. Press, NJ, 1994).
8. Carton, Y. & Bouletreau, M. Encapsulation ability of *Drosophila melanogaster*: a genetic analysis. *Dev. Comp. Immunol.* **9,** 211–219 (1985).
9. Carton, Y. & Nappi, A. J. The *Drosophila* immune reaction and the parasitoid capacity to evade it: genetic and coevolutionary aspects. *Acta Oecol.* **12,** 89–104 (1991).
10. Henter, H. J. & Via, S. The potential for coevolution in a host-parasitoid system. 1. Genetic variation within an aphid population in susceptibility to a parasitic wasp. *Evolution* **49,** 427–438 (1995).
11. Hughes, K. & Sokolowski, M. B. Natural selection in the laboratory for a change in resistance by *Drosophila melanogaster* to the parasitoid wasp *Asobara tabida. J. Insect Behav.* **9,** 477–491 (1996).
12. Kraaijeveld, A. R. & van der Wel, N. N. Geographic variation in reproductive success of the parasitoid *Asobara tabida* in larvae of several *Drosophila* species. *Ecol. Entomol.* **19,** 221–229 (1994).
13. Kraaijeveld, A. R. & van Alphen, J. J. M. Geographical variation in encapsulation ability of *Drosophila melanogaster* larvae and evidence for parasitoid-specific components. *Evol. Ecol.* **9,** 10–17 (1995).
14. Lewonton, R. C. The effects of population density and composition on viability in *Drosophila melanogaster. Evolution* **9,** 27–41 (1955).
15. Santos, M., Fowler, K. & Partridge, L. On the use of tester stocks to predict the competitive ability of genotypes. *Heredity* **69,** 489–495 (1992).
16. Atkinson, W. D. A field investigation of larval competition in domestic *Drosophila. J. Anim. Ecol.* **48,** 91–102 (1979).
17. McCullagh, P. & Nelder, J. A. *Generalized Linear Models* 2nd edn (Chapman & Hall, London, 1989).

Responses of primary visual cortical neurons to binocular disparity without depth perception

B. G. Cumming & A. J. Parker

University Laboratory of Physiology, Parks Road, Oxford OX1 3PT, UK

The identification of brain regions that are associated with the conscious perception of visual stimuli is a major goal in neuroscience[1]. Here we present a test of whether the signals on neurons in cortical area V1 correspond directly to our conscious perception of binocular stereoscopic depth. Depth perception requires that image features on one retina are first matched with appropriate features on the other retina. The mechanisms that perform this matching can be examined by using random-dot stereograms[2], in which the left and right eyes view randomly positioned but binocularly correlated dots. We exploit the fact that anticorrelated random-dot stereograms (in which dots in one eye are matched geometrically to dots of the opposite contrast in the other eye) do not give rise to the perception of depth[3] because the matching process does not find a consistent solution. Anti-correlated random-dot stereograms contain binocular features that could excite neurons that have not solved the correspondence problem. We demonstrate that disparity-selective neurons in V1 signal the disparity of anticorrelated random-dot stereograms, indicating that they do not unambiguously signal stereoscopic depth. Hence single V1 neurons cannot account for the conscious perception of stereopsis, although combining the outputs of many V1 neurons could solve the matching problem. The accompanying paper[4] suggests an additional function for disparity signals from V1: they may be important for the rapid involuntary control of vergence eye movements (eye movements that bring the images on the two foveae into register).

When the image of an object falls on different locations on the two retinae, this binocular disparity gives rise to a sensation of depth (stereopsis). This process requires that an image feature on one retina be matched with an appropriate feature on the other retina, even though there are inevitably similar features nearby offering potential matches. This problem is particularly apparent in random-dot stereograms (RDS), where there are many identical dots in both images. Of course it is not necessary to consider false matches in RDS on a dot-by-dot basis—spatial filtering of the image before matching can substantially reduce the number of false matches[5]. However, this filtering alone is insufficient to solve the correspondence problem and further computation is required to eliminate false matches. Consideration of the overall pattern of disparities can indicate which potential matches form a globally consistent pattern, and many computer algorithms achieve this[5,6].

Although single neurons in V1 have long been known to signal the disparity of a stimulus[7,8], their role in stereo matching is unclear. If they are directly responsible for the conscious perception of depth, they should respond only when matches within the receptive field are registered as globally correct. If binocular neurons respond equally well to false matches at appropriate disparities, then further processing (presumably outside V1) is required to account for the psychophysical ability to discard false matches.

Whether or not disparity-selective neurons respond only to correct matches is an open question. It has been demonstrated that some V1 complex cells display disparity selectivity to dynamic RDSs and it was concluded that these neurons signal "the correct binocular matches among a multitude of false matches ... (global
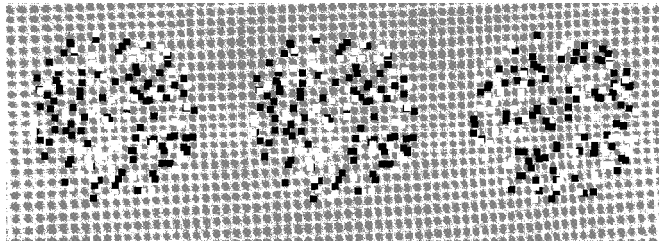
Figure 1 Example stereograms. The pair formed by the central image and the left image forms a C-RDS showing a central circular patch standing out in depth (shown for cross-eyed fusion). The pair formed by the central image and the right image is an A-RDS, and appears rivalrous with no consistent depth. Note that the right image is an exact copy of the left image in which the dot brightnesses have been reversed.

Figure 2 Responses of a model complex cell to RDS. The model neuron was tuned to zero-disparity stimuli. Filled symbols show responses to C-RDS, open symbols show responses to A-RDS. Both axes have arbitrary units. The model neuron had subunits that were matched in their spatial and temporal properties, so the two tuning curves are exact mirror images.

stereopsis)"[9]. However, even simple local matching may yield disparity-selective responses to these stimuli, because an identical pattern of dots lies at an appropriate location on each retina when the RDS is presented at an optimal disparity. Modelling confirms this quantitatively[10,11], but the success of such models is not evidence against global matching in V1: all of the current experimental evidence is equally compatible with the idea that V1 neurons actually perform a more complex analysis by solving the correspondence problem.

This question requires new experimental investigations. V1 neurons should be tested with stimuli for which the predictions of local filtering models are quite different from the pattern of responses that would be expected if neurons respond exclusively to global matches. One way to do this is to present local matches in the receptive field that do not correspond to correct global matches. This can be done using anticorrelated RDS (A-RDS) because the pattern of local matches they produce appears to be rivalrous with no consistent depth[2], except at low dot densities (<5%)[3]. The perceptual process behaves as if all these local matches are false matches (matches which are discarded by global stereopsis). We therefore compared the neuronal responses to anticorrelated and correlated RDS (C-RDS) in awake behaving monkeys.

The dynamic random dot patterns were composed of 50% black and 50% white dots against a grey background (Fig. 1). An anti-correlated stereogram was obtained by inverting the contrast of the image for one eye, so that each dot shown black to the right eye was shown white to the left eye, and vice versa. This has a predictable effect on disparity selectivity for the local filtering model: contrast reversal inverts the output of each monocular subunit, so contrast reversal of only one eye's image inverts the disparity tuning (see Methods). Figure 2 shows this inversion of disparity tuning for our implementation of a model complex cell[10,11]. So if single neurons perform only local stereoscopic matching, they should display an inverted disparity selectivity when tested with A-RDS. If they really perform global matching, they should not respond at all to A-RDS. Of course, the filter model could perhaps be elaborated so that it too could predict a failure to respond to A-RDS, but any positive experimental demonstration of disparity tuning to A-RDS must imply a failure to respond exclusively to globally correct matches.

Figure 3 shows the responses of two disparity-selective cells to dynamic A-RDS. The qualitative effects predicted by the model are
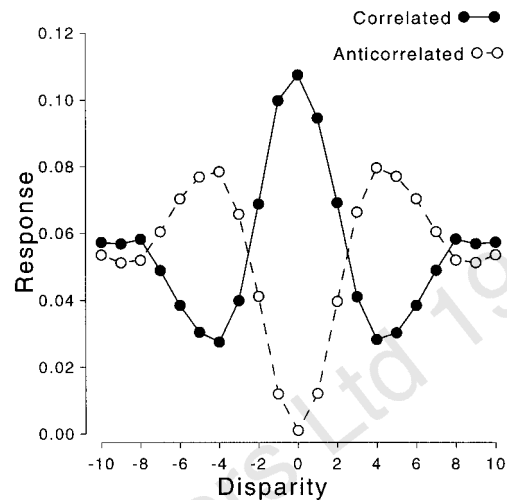
clearly seen: the neurons are disparity-selective to both stimuli, and the tuning curves are related by an inversion. Note that the responses to C-RDS are comparable to those reported by others[9,12]. To quantify these effects, disparity tuning curves were fitted with Gabor functions. The relationship between the two tuning curves for a single cell was characterized by two parameters: the difference in the fitted phase, and the ratio of the fitted amplitudes. Figure 3 shows these fitted curves superimposed on the neural data, and it can be seen that they provide a good description of the main features.

Quantitative disparity tuning data for both C-RDS and A-RDS were obtained on 72 disparity-selective neurons from two animals. These data are summarized in Fig. 4, which plots the ratio of the fitted amplitudes against the difference in the fitted phases. Most results cluster around the predicted phase difference (π), but the amplitude ratio was generally smaller than the predicted value (1.0). Indeed, a number of neurons essentially did not modulate their firing with the disparity of A-RDS. By itself this does not imply that these cells have solved the correspondence problem because this result can also be explained by more complex versions of the local filtering model. Conversely, any modulation of responses to A-RDS indicates strongly that the cells respond to false local matches. As the data in Fig. 4 do not show two distinct populations of neurons, the most parsimonious interpretation of these data is that binocular V1 neurons act as some form of local filter.

The importance of this result lies in the fact that it is incompatible with the claim that single V1 neurons have "the unique capacity of solving the correspondence problem"[13], an assertion that has not previously been critically tested. It is also incompatible with the view that these neurons perform matching dot-by-dot: in the anticorrelated stimulus, the white dots in one eye's image are uncorrelated with the white dots in the other eye's image. A scheme that matches the left edge of a white dot with the right edge of the corresponding black dot might explain the inverted responses, at least when the disparity is less than the dot width. However, such a scheme would produce responses that are not inverted for disparities greater than the dot width. We never observed such a response pattern, indeed the inverted responses were still evident at disparities much larger than the dot width (Fig. 3), as predicted by local spatial filtering.

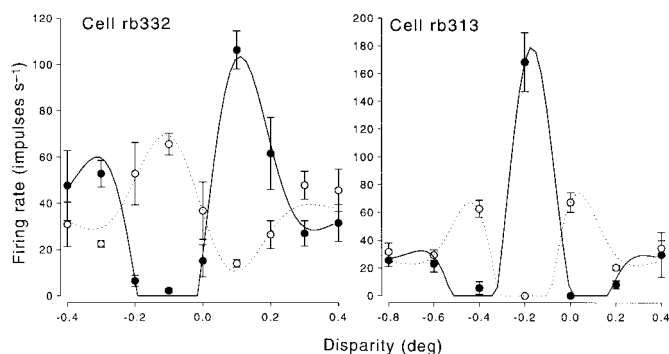In conclusion, most V1 neurons that show disparity selectivity for

Figure 3 Responses of two complex neurons to disparity in correlated (filled symbols) and anticorrelated (open symbols) dynamic RDS. Fitted curves for the two stimulus types are Gabor functions (see Methods), in which the only parameters that are permitted to differ are the phase and the amplitude. For the cell on the left, the phase difference was 0.95π and the ratio of the amplitudes was 0.36. For the cell on the right, these values were 0.86π and 0.68, respectively. Note that although the disparity tuning curves for the two cells are quite different, the relationship between the anticorrelated responses and the correlated responses is very similar, resembling the behaviour of the model. In both cases, the tuning curve to correlated patterns is inverted by anticorrelation. The dot size was 0.08 degrees.
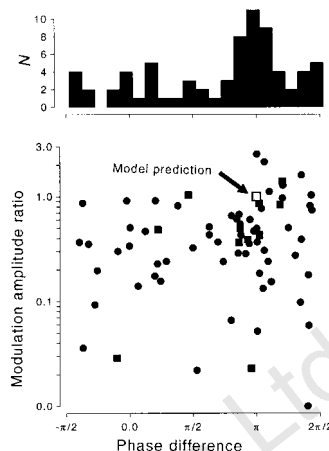

Figure 4 Summary of effect of stimulus anticorrelation on the disparity selectivity of 72 cells. Gabor functions were fitted to anticorrelated and correlated data for each cell (Fig. 3, and see Methods). In the lower panel the data from each cell are represented by a single point, which plots the relative amplitude of the fitted Gabors against the phase difference. Circles (60 cells) show results from the first animal, squares (12 cells) show results from a second. The model predicts a phase shift of π and an amplitude ratio of 1.0. Although the amplitude ratios are generally less than one (mean ratio, 0.52 ± 0.46 s.d.), most cells cluster around a phase shift of π. The upper panel shows a frequency histogram for the phase difference, confirming the existence of a cluster around π.

C-RDS also modulate their firing rate in response to disparity changes in A-RDS. The indicates that these neurons fail to distinguish reliably between global matches and false matches (local matches that are not global matches). One monkey (from whom the majority of neurons were recorded) was trained to perform psychophysical depth discrimination with RDS, but was not able to perform the discrimination with A-RDS. The fact that V1 neurons systematically alter their firing rate in response to stimulus manipulations that are not perceived psychophysically argues against a direct role for V1 neurons in binocular depth perception. As frequently suggested[14,15], these neurons may be involved in guiding vergence eye movements, a hypothesis that is tested in the accompanying paper examining short-latency vergence responses to A-RDS[4]. The failure to distinguish correct matches does not imply that V1 neurons have no role in stereo matching—the correct disparity matches could be extracted by combining the outputs of a number of these neurons. Our results indicate that this combination must occur outside V1. Applying the techniques described here in extrastriate cortex offers the opportunity of locating sites in the brain where stereo correspondence is achieved. □

Methods

Modelling. The model used to predict the responses of disparity-selective complex cells to dynamic RDS was our own implementation of the model described in ref. 10. Each eye's image is convolved with Gabor subunits in quadrature pairs. For each subunit, inputs from the two eyes are summed, and the binocular sum for each subunit is then squared (rectified) and summed to generate the complex cell output. The only difference between our model and that of ref. 10 was that we used positional displacements of the receptive fields to generate selectivity for different disparities, not phase differences. Both methods give similar results for RDS[11], and for the case of neurons tuned to zero disparity (Fig. 2) the two models are identical. For a model with N binocular subunits the response, R_c, to a correlated stimulus is given by:

$$R_c = \sum_{i=1}^{N} (l_i + r_i)^2 = \sum_{i=1}^{N} (l_i)^2 + \sum_{i=1}^{N} (r_i)^2 + 2\sum_{i=1}^{N} (r_i l_i)$$

where l_i and r_i are the outputs of left and right subunits, respectively. Inverting

the contrast of (for example) the right image inverts all of the terms r_i to give R_a, the response to the anticorrelated pattern:

$$R_c = \sum_{i=1}^{N} (l_i - r_i)^2 = \sum_{i=1}^{N} (l_i)^2 + \sum_{i=1}^{N} (r_i)^2 - 2\sum_{i=1}^{N} (r_i l_i)$$

The terms $\Sigma(l_i)^2$ and $\Sigma(r_i)^2$ describe the contents of the left and right images, and are not affected by changes in disparity. The term $\Sigma(r_i l_i)$, describes the relationship between the images in the two eyes, and gives rise to disparity selectivity. As this term is inverted by anticorrelation, the disparity tuning curve predicted by these models for anticorrelated RDS is an exact inversion of the tuning curve for correlated stimuli (Fig. 2). Note that this result does not depend upon there being a periodic receptive field: the same would be true if the subunits were simple gaussians, or any function where $f(-x) = -f(x)$.

Unit recording and stimulus presentation. Extracellular single-unit recordings were made in the primary visual cortex of two alert monkeys (*Macaca mulatta*). Scleral search coils were implanted[16] in both eyes under general anaesthesia, together with a head holder and a recording chamber. Animals were then trained to maintain binocular fixation. Tungsten-in-glass microelectrodes were introduced transdurally each day into the primary visual cortex. All procedures complied with the UK Home Office regulations on animal experimentation.

Receptive field eccentricity ranged from 1 to 4 degrees. Spike waveforms and eye-position traces were recorded to disk using the Datawave Discovery package, so that unit isolation and binocular fixation could be checked off-line. Mean firing rate was used to assess the unit response, summing all of the spikes that occurred from a time 50 ms after the first video frame of the stimulus was presented until 50 ms after the last video frame was presented.

Random-dot stimuli, like those shown in Fig. 1 (but dynamic, with a new dot pattern every 72 Hz video frame), were generated on a Silicon Graphics Indigo workstation, and displayed on two Tektronix GMA201 greyscale monitors through a haploscope. The dot width was usually 0.08 degrees (in a few simple cells it was necessary to use larger dots), the dot density was 25%, and the stimulus duration was 2 s. The stereogram always consisted of a background region at zero disparity, and a foreground region whose disparity was varied from trial to trial. Correlated and anticorrelated stimuli were alternated, but the sequence of disparities was randomized. Before testing units with RDS, the minimum response field was determined using flashing

black-and-white bars at the neuron's preferred orientation. The central region of the stereogram completely covered the minimum response field. After testing with RDS, neurons were classified as simple or complex on the basis of the modulation in their firing to drifting gratings[17]. Of the 72 neurons, 57 were tested in this way, of which 50 were complex cells and 7 were simple cells.

Analysis. For each neuron, the mean firing rate as a function of disparity ($f(d)$) was fitted with a Gabor function:

$$f(d) = A \exp(-(d-D)^2/2\sigma^2)\cos(2\pi\omega(d-D)+\phi)+B$$

by nonlinear regression, where A, ω and ϕ are the amplitude, spatial frequency and phase, respectively, of the cosine component, σ is the standard deviation of the gaussian, D is a position offset, and B is the baseline firing rate. In our model, this baseline firing corresponds to the activity produced by uncorrelated random-dot patterns. The correlated and anticorrelated data were fitted simultaneously, using the same values of B, ω, σ and D, but different values of A and ϕ (A_c, A_a, ϕ_c, ϕ_a, where the subscripts c and a refer to correlated and anticorrelated fits, respectively). The way in which changing from correlated to anticorrelated stimuli altered the disparity tuning of a single neurons could therefore be summarized by two parameters: an amplitude ratio A_a/A_c and a phase difference $\phi_c - \phi_a$. For the model complex cell, the amplitude ratio was 1.0 and the phase difference was π.

1. Crick, F. & Koch, C. Are we aware of neural activity in primary visual cortex? *Nature* **375**, 121–123 (1995).
2. Julesz, B. *Foundations of Cyclopean Perception* (University of Chicago Press, 1971).
3. Cogan, A. I., Lomakin, A. J. & Rossi, A. Depth in anticorrelated stereograms. *Vision Res.* **33**, 1959–1975 (1993).
4. Masson, G. S., Busettini, C. & Miles, F. A. Vergence eye movements in response to binocular disparity without depth perception. *Nature* **389**, 283–286 (1997).
5. Marr, D. & Poggio, T. A computatonal theory of human stereo vision. *Proc. R. Soc. Lond. B* **204**, 301–328 (1979).
6. Grimson, W. E. L. A computer implementation of a theory of human stereo vision. *Phil. Trans. R. Soc. Lond. B* **292**, 217–253 (1981).
7. Barlow, H. B., Blakemore, C. & Pettigrew, J. D. The neural mechanisms of binocular depth discrimination. *J. Physiol. (Lond.)* **193**, 327–342 (1967).
8. Nikara, T., Bishop, P. O. & Pettigrew, J. D. Analysis of retinal correspondence by studying receptive fields of binocular single units in cat striate cortex. *Exp. Brain Res.* **6**, 353–372 (1968).
9. Poggio, G., Motter, B. C., Squatrito, S. & Trotter, Y. Responses of neurons in visual cortex (V1 and V2) of the alert macaque to dynamic random dot stereograms. *Vision Res.* **25**, 397–405 (1985).
10. Ohzawa, I., DeAngelis, G. C. & Freeman, R. D. Stereoscopic depth discrimination in the visual cortex: Neurons ideally suited as disparity detectors. *Science* **249**, 1037–1041 (1990).
11. Qian, N. Computing stereo disparity and motion with known binocular properties. *Neural Computat.* **6**, 390–404 (1994).
12. Poggio, G. F., Gonzalez, F. & Krause, F. Stereoscopic mechanisms in monkey visual cortex: binocular correlation and disparity selectivity. *J. Neurosci.* **8**, 4531–4550 (1988).
13. Poggio, G. & Poggio, T. The analysis of stereopsis. *Annu. Rev. Neurosci.* **7**, 379–412 (1984).
14. Poggio, G. F. & Fisher, B. Binocular interactions and depth sensitivity in striate and prestriate cortex of behaving rhesus monkey. *J. Neurophysiol.* **40**, 1392–1405 (1977).
15. Poggio, G. Mechanisms of stereopsis in monkey visual cortex. *Cerebr. Cort.* **3**, 193–204 (1995).
16. Judge, S. J., Richmond, B. J. & Chu, F. C. Implantation of magnetic search coils for measurement of eye position: an improved method. *Vision Res.* **30**, 535–538 (1980).
17. Skottun, B. C. *et al.* Classifying simple and complex cells on the basis of response modulation. *Vision Res.* **31**, 1079–1086 (1991).

Vergence eye movements in response to binocular disparity without depth perception

G. S. Masson*, C. Busettini & F. A. Miles

Laboratory of Sensorimotor Research, National Eye Institute, National Institutes of Health, Bethesda, Maryland 20892, USA
* Centre de Recherche en Neurosciences Cognitives, Centre National de la Recherche Scientifique, 13402 Marseille, France

Primates use vergence eye movements to align their two eyes on the same object and can correct misalignments by sensing the difference in the positions of the two retinal images of the object (binocular disparity). When large random-dot patterns are viewed dichoptically and small binocular misalignments are suddenly imposed (disparity steps), corrective vergence eye movements are elicited at ultrashort latencies[1,2]. Here we show that the same steps applied to dense anticorrelated patterns, in which each black dot in one eye is matched to a white dot in the other eye, initiate vergence responses that are very similar, except that they are in the opposite direction. This sensitivity to the disparity of anticorrelated patterns is shared by many disparity-selective neurons in cortical area V1 (ref. 3), despite the fact that human subjects fail to perceive depth in such stimuli[4,5]. These data indicate that the vergence eye movements initiated at ultrashort latencies result solely from locally matched binocular features, and derive their visual input from an early stage of cortical processing before the level at which depth percepts are elaborated.

Disparity-selective neurons have often been implicated in the perception of depth (stereopsis)[6], and it has been shown that in the first stage of the cortical visual pathways in area V1, such neurons are sensitive to the disparity of anticorrelated patterns[3], even though such patterns are perceptually rivalrous, cannot be fused, and lack consistent depth[4,5]. Furthermore, the disparity tuning curves of the neurons were often inverted with anticorrelated patterns, a characteristic of simple local filtering models[7,8]. These findings are consistent with the hypothesis that these neurons respond to purely local matches between the images seen by the two eyes, regardless of whether a global match is present[9]. Thus, such neurons do not solve the correspondence problem and can represent only a rudimentary stage in the processing of binocular signals for stereopsis. We now provide evidence that such rudimentary binocular signals can generate motor responses by showing that small disparity stimuli applied to dense anticorrelated patterns give rise to inverted vergence eye movements at ultrashort latencies.

A variety of cues can be used to control the angle of convergence between the two lines of sight[10,11], but the only cue of concern here is binocular disparity[1,12], which provides a direct measure of the misalignment of the two eyes with respect to the object(s) of interest (vergence error) and is assumed to be sensed directly by disparity-selective neurons[13,14]. Examples of the initial vergence responses elicited by small horizontal disparities ($<2°$) applied to large correlated random-dot patterns (matching images at the two eyes) are seen in Fig. 1 (continuous line), which shows mean vergence velocity profiles for one human (Fig. 1a) and for one monkey (Fig. 1c). Stimuli were presented on a tangent screen using two slide projectors and orthogonal polarizing filters to allow independent control of the images seen by each eye. Each trial started with the screen blank and then stationary patterns with a given horizontal disparity were presented. For the data shown in Fig. 1a, c, all patterns had crossed disparities (the pattern seen by the right eye had been shifted leftwards; the pattern seen by the left eye had been shifted rightwards), simulating the abrupt appearance of a textured surface in front of the tangent screen. Such stimuli initiated increased convergence—the correct response to restore binocular alignment—with a latency of <60 ms in the case of the monkey and <90 ms in the case of the human[1,2]. The initial vergence responses to anticorrelated random-dot patterns with similar crossed disparities are shown as dotted lines in Fig. 1a, c and are clearly in the reverse direction. These inverted responses have a comparably short latency but a slightly lower rate of acceleration.

We quantified these initial motor responses by measuring the change in vergence position over a 33-ms period commencing at a fixed time after the appearance of the disparity stimuli: 60 ms for the monkey, 90 ms for the human. This meant that our measures were restricted to the initial (open-loop) vergence responses that were generated by the disparity input before it had been affected by eye-movement feedback. Disparity tuning curves based on these measures are plotted in Fig. 1b (human) and Fig. 1d (monkey), and show the characteristic S-shapes with non-zero asymptotes[1], consistent with the operation of a depth-tracking servo of modest range. Thus, with normal (correlated) patterns and disparities up to a degree or two, the slopes are positive and small increases in the